Available online at www.sciencedirect.com
ScienceDirect
Journal of Organometallic Chemistry 691 (2006) 4725–4732
Journal of Organometallic Chemistry
www.elsevier.com/locate/jorganchem

Synthesis, crystal structure, phase transition and thermal behaviour of a new dabcodiium hexaaquanickel(II) bis(sulphate), $(C_6H_{14}N_2)[Ni(H_2O)_6](SO_4)_2$

W. Rekik [a,b], H. Naïli [a,*], T. Bataille [b], T. Mhiri [a]

[a] *Laboratoire de l'Etat Solide, Département de Chimie, Faculté des Sciences de Sfax, BP 802, 3018 Sfax, Tunisia*
[b] *Sciences Chimiques de Rennes (CNRS, UMR 6226), Groupe Matériaux Inorganiques: Chimie Douce et Réactivité, Université de Rennes I, Avenue du Général Leclerc, 35042 Rennes Cedex, France*

Received 12 June 2006; received in revised form 15 July 2006; accepted 16 July 2006
Available online 28 July 2006

Abstract

A new dabcodiium-templated nickel sulphate, $(C_6H_{14}N_2)[Ni(H_2O)_6](SO_4)_2$, has been synthesised and characterised by single-crystal X-ray diffraction at 20 and −173 °C, differential scanning calorimetry (DSC), thermogravimetry (TG) and temperature-dependent X-ray powder diffraction (TDXD). The high temperature phase crystallises in the monoclinic space group $P2_1/n$ with the unit-cell parameters: $a = 7.0000(1)$, $b = 12.3342(2)$, $c = 9.9940(2)$ Å; $\beta = 90.661(1)°$, $V = 862.82(3)$ Å^3 and $Z = 2$. The low temperature phase crystallises in the monoclinic space group $P2_1/a$ with the unit-cell parameters: $a = 12.0216(1)$, $b = 12.3559(1)$, $c = 12.2193(1)$ Å; $\beta = 109.989(1)°$, $V = 1705.69(2)$ Å^3 and $Z = 4$. The crystal structure of the HT-phase consists of Ni^{2+} cations octahedrally coordinated by six water molecules, sulphate tetrahedra and disordered dabcodiium cations linked together by hydrogen bonds. It undergoes a reversible phase transition (PT) of the second order at −53.7/−54.6 °C on heating–cooling runs. Below the PT temperature, the structure is fully ordered. The thermal decomposition of the precursor proceeds through three stages giving rise to the nickel oxide.

Keywords: Chemical synthesis; Crystal structure; Phase transition; Order–disorder; Thermal behaviour; Organometallic

1. Introduction

The chemistry of organically templated metal sulphate has received increasing attention over the last few years. A great interest has been shown in some double sulphates of trivalent metal with monovalent aliphatic ammonium cations because of their ferroelastic and ferroelectric properties [1–5]. So far, there are few data on double sulphates of divalent metal cation with mono or divalent organic cations [6–21]. In order to expand the emergent chemistry of double sulphates of transition metal with diamine and to obtain crystals exhibiting ferroelectric or ferroelastic properties, a new compound using 1,4-diazabicyclo[2.2.2]octane (hereafter referred to as dabcodiium) as a template and nickel as transition metal has been synthesised. In this paper, we report the chemical preparation, the crystal structure determination, the phase transition and the thermal behaviour of the two phases of the title compound (further referred to as the HT- and LT-phases).

2. Experimental

2.1. Synthesis

Transparent green crystals of dabcodiium hexaaquanickel(II) bis(sulphate), $(C_6H_{14}N_2)[Ni(H_2O)_6](SO_4)_2$, were grown by slow evaporation at room temperature from an aqueous solution containing $NiSO_4 \cdot 6H_2O$, $C_6H_{12}N_2$ and H_2SO_4 in equimolar ratio. The single crystals were recrystallised and the product was filtered off and washed with a small amount of distilled water.

* Corresponding author. Tel.: +216 98 660 026; fax: +216 74 274 437.
E-mail address: houcine_naili@yahoo.com (H. Naïli).

0022-328X/$ - see front matter © 2006 Elsevier B.V. All rights reserved.
doi:10.1016/j.jorganchem.2006.07.019

2.2. Single-crystal data collection and structure determination

Suitable crystals of the title compound were glued to a glass fibre mounted on a four-circle Nonius KappaCCD area-detector diffractometer. Intensity data sets were collected using Mo Kα ($\lambda = 0.71073$ Å) with the program COLLECT [22]. Correction for Lorentz-polarisation effect, peak integration and background determination was carried out with the program DENZO [23]. Frame scaling and unit cell parameters refinement were performed with the program SCALEPACK [23]. Numerical absorption correction was performed by modelling the crystal faces [24]. Crystallographic data at 20 and −173 °C are listed in Table 1.

Both phases were found to crystallise in monoclinic symmetry in the same space group. However, in order to avoid an unusually large monoclinic angle, we assigned the space group settings $P2_1/n$ for the compound at 20 °C and $P2_1/a$ for the compound at −173 °C, called hereafter HT and LT phases, respectively. Nickel and sulphur atoms were located using direct methods with the program SHELXS-97 [25]. The oxygen atoms and the organic moieties were found from successive difference Fourier calculations using SHELXL-97 [26]. For the room temperature phase, all H atoms were located by difference Fourier syntheses after several cycles of least-squares refinements. H–O and H–H distances, within water molecules, were restrained to 0.85(2) and 1.39(2) Å, respectively. C–H and H–H distances within the disordered organic moiety were also restrained to 0.97(2) and 1.58(4) Å, respectively, so that the H–C–H angles fitted the ideal values of the tetrahedral angle. In the LT-phase, the H atoms bonded to N and O were located in a difference Fourier map and their positions and isotropic displacement parameters were refined. H–O and H–H distances, within water molecules, were restrained to 0.85(2) and 1.35(2) Å, respectively. H atoms bonded to C atoms were positioned geometrically (the C–H bonds were fixed at 0.97 Å) and allowed to "ride" on their parent atoms. The atomic coordinates and isotropic displacement parameters are given in Table 2. Bond distances and angles calculated from the final atomic coordinates, as well as probable hydrogen bonds, are given in Tables 3 and 4.

Further details of the crystal structure investigations at −173 °C and 20 °C can be obtained from the Cambridge Crystallographic Data Centre. The deposition numbers are CCDC 604491 and CCDC 604492.

2.3. Thermal behaviour

Differential scanning calorimetry at low temperature was performed with a SETARAM DSC131 instrument for temperatures ranging from −150 to 37 °C at a rate of 5 °C min^{-1}. A polycrystalline sample of 27.85 mg was placed in a hermetic aluminium cell in the nitrogen atmosphere.

Table 1
Crystallographic data for $(C_6H_{14}N_2)[Ni(H_2O)_6](SO_4)_2$

Empirical formula	$C_6H_{26}N_2NiO_{14}S_2$	$C_6H_{26}N_2NiO_{14}S_2$
Formula weight	473.12	473.12
Temperature (°C)	20(2)	−173(2)
Crystal system	Monoclinic	Monoclinic
Space group	$P2_1/n$	$P2_1/a$
a (Å)	7.0000(1)	12.0216(1)
b (Å)	12.3342(2)	12.3559(1)
c (Å)	9.9940(2)	12.2193(1)
β (°)	90.661(1)	109.989(1)
V (Å^3)	862.82(3)	1705.69(2)
Z	2	4
ρ_{cal} (g cm^{-1})	1.821	1.842
Crystal size (mm^3)	$0.400 \times 0.308 \times 0.277$	$0.354 \times 0.300 \times 0.279$
Habit-colour	Prism-green	Prism-green
λ (Mo Kα) (Å)	0.71073	0.71073
μ (mm^{-1})	1.440	1.457
θ Range (°)	2.62–32.06	3.30–42.21
Index ranges	$-10 \leqslant h \leqslant 9$, $-18 \leqslant k \leqslant 18$, $-14 \leqslant l \leqslant 14$	$-22 \leqslant h \leqslant 22$, $-23 \leqslant k \leqslant 22$, $-23 \leqslant l \leqslant 23$
Unique data	3005	12021
Observed data [$I > 2\sigma(I)$]	2643	9965
F(000)	496	992
Extinction coefficient	0.216(8)	0.0178(8)
Refinement method	Full matrix least-squares on $\|F^2\|$	Full matrix least-squares on $\|F^2\|$
R_1	0.0368	0.0327
WR_2	0.1007	0.0868
Goodness-of-fit (GOF)	1.072	1.052
Number of parameters	219	283
Transmission factors	0.61234 and 0.75326	0.61645 and 0.73536
Largest difference map hole and peak (e Å^{-3})	−0.827 and 0.875	−1.139 and 1.010

Table 2
Fractional atomic coordinates and equivalent isotropic temperature factor (Å^2) with esd's in parentheses

Atom	x	y	z	U_{eq}[a]
$(C_6H_{14}N_2)[Ni(H_2O)_6](SO_4)_2$ (20 °C)				
Ni	0.0000	0.0000	0.0000	0.0219(1)
S	−0.01406(5)	0.25662(3)	0.36826(4)	0.0276(1)
OW1	0.2104(2)	−0.0844(1)	−0.0932(1)	0.0312(2)
OW2	0.2106(2)	0.0817(1)	0.1009(1)	0.0312(2)
OW3	0.0005(2)	−0.0038(1)	0.1582(1)	0.0364(3)
O1	−0.0408(2)	0.1724(1)	0.4694(2)	0.0596(5)
O2	−0.0079(2)	0.3640(1)	0.4323(1)	0.0356(3)
O3	0.1670(2)	0.2393(1)	0.2978(2)	0.0373(3)
O4	−0.1772(2)	0.2539(1)	0.2735(2)	0.0469(4)
N	−0.3596(2)	0.05613(1)	0.4714(2)	0.0370(3)
C1	−0.3084(6)	−0.0388(4)	0.5277(7)	0.058(1)
C2	−0.5208(6)	0.1134(3)	0.4498(6)	0.047(1)
C3	−0.3434(5)	−0.0499(3)	0.3920(3)	0.0343(7)
C4	−0.5009(7)	0.1247(3)	0.5579(4)	0.0439(9)
C5	−0.3299(5)	0.0184(3)	0.6211(4)	0.0321(6)
C6	−0.4869(6)	0.0393(4)	0.3396(4)	0.0442(9)
$(C_6H_{14}N_2)[Ni(H_2O)_6](SO_4)_2$ (−173 °C)				
Ni	0.741088(8)	0.495436(7)	0.248052(8)	0.00828(3)
S1	0.43237(2)	0.75153(1)	0.05975(2)	0.00847(3)
S2	0.07834(2)	0.26909(1)	0.43907(2)	0.00907(3)
OW1	0.68625(5)	0.57741(5)	0.09476(5)	0.01211(9)
OW2	0.80234(5)	0.41051(5)	0.39995(5)	0.01177(9)
OW3	0.58266(5)	0.41510(5)	0.19392(5)	0.01220(9)
OW4	0.89822(5)	0.57796(5)	0.30392(5)	0.01203(9)
OW5	0.82091(5)	0.38112(5)	0.16970(5)	0.01273(9)
OW6	0.66027(6)	0.60884(5)	0.32760(6)	0.0144(1)
O1	0.47681(6)	0.83483(5)	−0.00158(5)	0.0162(1)
O2	0.46224(5)	0.64201(5)	0.02929(5)	0.0133(1)
O3	0.48689(5)	0.76692(5)	0.18727(5)	0.01204(9)
O4	0.30155(5)	0.76057(5)	0.02337(5)	0.0128(1)
O5	0.04981(6)	0.18244(5)	0.50827(6)	0.0170(1)
O6	0.01786(6)	0.24849(5)	0.31330(5)	0.0137(1)
O7	0.03804(5)	0.37478(5)	0.46909(5)	0.01193(9)
O8	0.20857(5)	0.27320(5)	0.46567(6)	0.0150(1)
N1	0.29427(6)	0.56495(5)	0.33284(6)	0.0113(1)
N2	0.18458(6)	0.45129(5)	0.16183(6)	0.0111(1)
C1	0.17591(7)	0.53776(7)	0.34013(7)	0.0143(1)
C2	0.36317(8)	0.46390(7)	0.33420(8)	0.0185(2)
C3	0.27778(8)	0.62718(6)	0.22319(7)	0.0148(1)
C4	0.28567(7)	0.38728(6)	0.23993(8)	0.0162(1)
C5	0.23049(7)	0.54980(6)	0.11952(7)	0.0133(1)
C6	0.10273(7)	0.48404(6)	0.22515(7)	0.0126(1)

[a] U_{eq} is defined as one-third of trace of the orthogonalized U_{ij} tensor.

A thermogravimetric (TG) measurement was performed with a Rigaku Thermoflex instrument under flowing air, with a heating rate of 15 °C h^{-1} from ambient temperature to 900 °C. The powdered sample, 11.47 mg, was spread evenly in a large platinium crucible to avoid mass effects.

Temperature-dependent X-ray powder diffraction (TDXD) was performed with a powder diffractometer combining the curved-position-sensitive detector (CPS120) from INEL and a high temperature attachment from Rigaku. The detector was used in a semi-focusing arrangement by reflection (Cu Kα_1 radiation, $\lambda = 1.5406$ Å) as described elsewhere [27]. The thermal decomposition of the title compound was carried out in flowing air with a heating rate of 7 °C h^{-1} from 24 °C until 610 °C.

3. Results

3.1. Thermal behaviour

A DSC experiment including heating and cooling processes between −150 and 37 °C is shown in Fig. 1. The calorimetric measurements show that, up to 37 °C, one reversible phase transition of the second order is observed at −53.7/−54.6 °C on heating–cooling runs. The characteristic thermodynamic values have been determined as follows:

Increasing temperature	Decreasing temperature
T_o (onset) = −53.7 ± 0.3 °C	T_o (onset) = −54.6 ± 0.3 °C
T_s (peak) = −53.1 ± 0.3 °C	T_s (peak) = −55.2 ± 0.3 °C
$\Delta H = 371.5$ J mol^{-1}	$\Delta H = -360.8$ J mol^{-1}
$\Delta S = 1.689$ J mol^{-1} K^{-1}	$\Delta S = 1.656$ J mol^{-1} K^{-1}

The shape of the heat anomaly and relatively small thermal hysteresis of about 1 °C clearly indicate the continuous nature of the phase transition.

The TG analysis (Fig. 2) shows that the dehydration occurs in the temperature range 92–137 °C and corresponds to the departure of the six water molecules (observed and theoretical weight losses, 22.2% and 22.8%). Fig. 3 shows the three-dimensional representation of the powder diffraction patterns obtained during the decomposition of $(C_6H_{14}N_2)[Ni(H_2O)_6](SO_4)_2$ under flowing air in the temperature range 24–610 °C. This plot reveals that the precursor is stable until 92 °C and then transforms into the anhydrous phase, $(C_6H_{14}N_2)Ni(SO_4)_2$, amorphous to X-rays. The anhydrous compound, pointed out with the first plateau observed on the TG curve, is stable between 137 and 255 °C. The second transformation starts at 255 °C and corresponds to the decomposition of the amine entity and the partial decomposition of the sulphate groups. Consequently, the given product is a mixture of crystallised $NiSO_4$ and NiO phases, as also confirmed by the TDXD plot at 460 °C. The end of the decomposition is marked by a plateau at 685 °C corresponding to the total decomposition of $NiSO_4$ into NiO according to the observed weight loss of 83.3% (calculated weight loss, 84.2%).

3.2. Description of the structures

3.2.1. Structure of the HT-phase (determined at 20 °C)

The structure of the title compound consists of Ni^{2+} cations octahedrally coordinated by six water molecules, sulphate tetrahedra and disordered dabcodiium cations linked together by hydrogen bonds only (Fig. 4a). The Ni(II) atoms are located in special positions (0 0 0) and (1/2 1/2 1/2) on inversion centres. Each of them is sixfold coordinated by six water-molecule oxygen atoms from which three are crystallographically independent. These $[Ni(H_2O)_6]^{2+}$ octahedra are slightly distorted. In fact, the Ni–OW distances range from 2.038(1) to 2.114(1) Å and

Table 3
Selected bond distances (Å) and angles (°)

Octahedron around Ni		Tetrahedron around S		Within the organic moiety	
$(C_6H_{14}N_2)[Ni(H_2O)_6](SO_4)_2$ (20 °C)					
Ni–OW1	2.038(1)	S1–O1	1.463(2)	N–C1	1.346(5)
Ni–OW2	2.042(1)	S1–O2	1.472(1)	N–C2	1.347(4)
Ni–OW3	2.114(1)	S1–O3	1.472(1)	N–C3	1.534(4)
OW1–Ni–OW2	87.49(5)	S1–O4	1.476(1)	N–C4	1.569(4)
OW1–Ni–OW2^{I}	92.51(5)	O1–S1–O2	110.0(1)	N–C5	1.579(4)
OW1–Ni–OW3	90.45(5)	O1–S1–O3	110.18(9)	N–C6	1.595(4)
OW1–Ni–OW3^{I}	89.55(5)	O1–S1–O4	108.9(1)	C1–C2^{I}	1.528(6)
OW2–Ni–OW3	87.91(5)	O2–S1–O3	108.50(7)	C4–C3^{I}	1.517(5)
OW2–Ni–OW3^{I}	92.09(5)	O2–S1–O4	108.55(8)	C6–C5^{I}	1.521(5)
		O3–S1–O4	110.72(9)	C2–N–C3	115.6(3)
				C2–N–C5	114.0(3)
				C3–N–C5	103.2(2)
				C1–N–C4	113.9(3)
				C1–N–C6	112.1(3)
				C4–N–C6	100.1(3)
				N–C1–C2^{I}	112.4(3)
				N–C4–C3^{I}	108.3(3)
				N–C6–C5^{I}	108.2(3)

Symmetry codes: $^{I} -x-1, -y, -z+1$

Octahedron around Ni		Tetrahedron around S(1)		Within the organic moiety	
$(C_6H_{14}N_2)[Ni(H_2O)_6](SO_4)_2$ (−173 °C)					
Ni–OW1	2.0310(6)	S1–O1	1.4765(6)	N1–C1	1.494(1)
Ni–OW2	2.0381(6)	S1–O2	1.4798(6)	N1–C2	1.495(1)
Ni–OW3	2.0467(6)	S1–O3	1.4817(6)	N1–C3	1.498(1)
Ni–OW4	2.0475(6)	S1–O4	1.4851(6)	N2–C4	1.490(1)
Ni–OW5	2.1120(6)	O1–S1–O2	110.41(4)	N2–C5	1.500(1)
Ni–OW6	2.1208(6)	O1–S1–O3	109.73(4)	N2–C6	1.500(1)
OW1–Ni–OW2	177.41(2)	O1–S1–O4	109.00(4)	C1–C6	1.531(1)
OW1–Ni–OW3	88.34(2)	O2–S1–O3	108.89(3)	C2–C4	1.535(1)
OW1–Ni–OW4	91.76(2)	O2–S1–O4	108.46(3)	C3–C5	1.533(1)
OW1–Ni–OW5	88.28(2)	O3–S1–O4	110.34(4)	C1–N1–C2	110.29(7)
OW1–Ni–OW6	92.19(3)	Tetrahedron around S(2)		C1–N1–C3	109.34(6)
OW2–Ni–OW3	92.93(2)	S2–O5	1.4755(6)	C2–N1–C3	109.99(7)
OW2–Ni–OW4	87.01(2)	S2–O6	1.4803(6)	C4–N2–C5	109.63(6)
OW2–Ni–OW5	89.41(2)	S2–O7	1.4819(6)	C4–N2–C6	110.36(6)
OW2–Ni–OW6	90.13(2)	S2–O8	1.4871(6)	C5–N2–C6	110.02(6)
OW3–Ni–OW4	178.86(2)	O5–S2–O6	110.02(4)	N1–C1–C6	107.64(6)
OW3–Ni–OW5	92.63(2)	O5–S2–O7	109.75(4)	N1–C2–C4	108.34(6)
OW3–Ni–OW6	86.96(2)	O5–S2–O8	109.46(4)	N1–C3–C5	108.50(6)
OW4–Ni–OW5	88.50(2)	O6–S2–O7	108.81(3)	N2–C4–C2	107.83(6)
OW4–Ni–OW6	91.90(2)	O6–S2–O8	109.85(4)	N2–C5–C3	107.32(6)
OW3–Ni–OW6	179.38(2)	O7–S2–O8	108.94(3)	N2–C6–C1	108.53(6)

the *cis*-OW–Ni–OW angles vary from 87.49(5) to 92.51(5)° (Table 3). The Ni atoms are isolated from any others with a shortest Ni–Ni distance 7.00 Å. The octahedra run along the *a* and *c* axes, forming inorganic cationic stacks along [1 0 0] and [0 0 1]. Each octahedron is H-bonded to six sulphate anions in a bidentate fashion.

The dabcodiium groups are located around inversion centres at (1/2 0 1/2) and (0 1/2 0), while all their atoms are located in general positions. Their internal symmetry, D_{3h}, does not contain any inversion centre. Consequently, the molecule adopts two possible orientations. The C atoms are distributed between two positions related by the symmetry centre, with a refined site occupancy factor equal to 0.5. Two possible models can be attributed to this disorder: static disordering in two positions or dynamical disordering of all the dabcodiium ions turning through 180° around any axis that passes through the inversion centre and perpendicular to the N–N axis. It is well known that the X-ray diffraction experiment does not allow to determine which of the indicated models is true. In order to find out the correct model, dielectric studies are required. Fig. 5a shows the two possible orientations of the dabcodiium group. Within the dabcodiium cations, the N–C distances and the C–N–C angles range from 1.346(5) to 1.595(4) Å and from 100.1(3) to 115.6(3)°, respectively (Table 3). Also, the values in the present structure deviate most strongly from those in the literature [28], especially the C–N-distances. These deviations are probably due to the disorder of the carbon atoms. The organic cations occupy the same positions as the metallic octahedra translated by half the *b* axis, so that they are placed in the middle of the edge parallel to the b axis and the centres of

Table 4
Hydrogen-bonding geometry (Å, °)

D–H···A	*d*(D–H) (Å)	*d*(H···A) (Å)	*d*(D···A) (Å)	∠D–H···A (°)
$(C_6H_{14}N_2)[Ni(H_2O)_6](SO_4)_2$ (20 °C)				
N–HN···O1	0.96(3)	1.72(3)	2.653(2)	162(2)
OW1–H11···O4^{I}	0.86(2)	1.92(2)	2.768(2)	169(3)
OW1– H12···O2^{II}	0.88(2)	1.81(2)	2.692(2)	176(3)
OW2–H21···O3	0.86(2)	1.94(2)	2.786(2)	168(3)
OW2–H22···O2^{III}	0.87(2)	1.83(2)	2.692(2)	173(3)
OW3–H31···O4^{IV}	0.85(2)	2.03(2)	2.878(2)	174(2)
OW3–H32···O3^{II}	0.85(2)	2.13(2)	2.979(2)	179(2)
Symmetry codes: $^{I}-x,-y,-z$; $^{II}-x+1/2,y-1/2,-z+1/2$; $^{III}x+1/2,-y+1/2,z-1/2$; $^{IV}-x-1/2,y-1/2,-z+1/2$.				
$(C_6H_{14}N_2)[Ni(H_2O)_6](SO_4)_2$ (−173 °C)				
N1–HN1···O5^{VII}	0.89(1)	1.75(1)	2.6273(9)	169(1)
N2–HN2···O1^{VI}	0.88(1)	1.80(1)	2.6592(9)	167(1)
OW1–H11···O4^{V}	0.83(1)	1.91(1)	2.7416(8)	173(2)
OW1– H12···O2	0.86(1)	1.80(1)	2.6564(8)	178(2)
OW2–H21···O7^{II}	0.84(1)	1.87(1)	2.7020(8)	176(2)
OW2–H22···O8^{III}	0.85(1)	1.92(1)	2.7726(8)	174(2)
OW3–H31···O6^{III}	0.83(1)	1.93(1)	2.7562(8)	172(2)
OW3–H32···O2^{IV}	0.83(1)	1.86(1)	2.6874(8)	175(2)
OW4–H41···O7^{I}	0.84(1)	1.84(1)	2.6774(8)	175(2)
OW4–H42···O3^{V}	0.85(1)	1.98(1)	2.8072(8)	168(2)
OW5–H51···O4^{IV}	0.84(1)	2.07(1)	2.9023(8)	178(2)
OW5–H52···O6^{II}	0.85(1)	2.07(1)	2.9207(8)	178(1)
OW6–H61···O8^{I}	0.83(1)	2.05(1)	2.8755(9)	179(2)
OW6–H62···O3	0.84(1)	2.10(1)	2.9421(8)	178(1)
Symmetry codes: $^{I}-x+1,-y+1,-z+1$; $^{II}x+1,y,z$; $^{III}x+1/2,-y+1/2,z$; $^{IV}-x+1,-y+1,-z$; $^{V}x+1/2,-y+3/2,z$; $^{VI}-x+1/2,y-1/2,-z$; $^{VII}-x+1/2,y+1/2,-z+1$.				

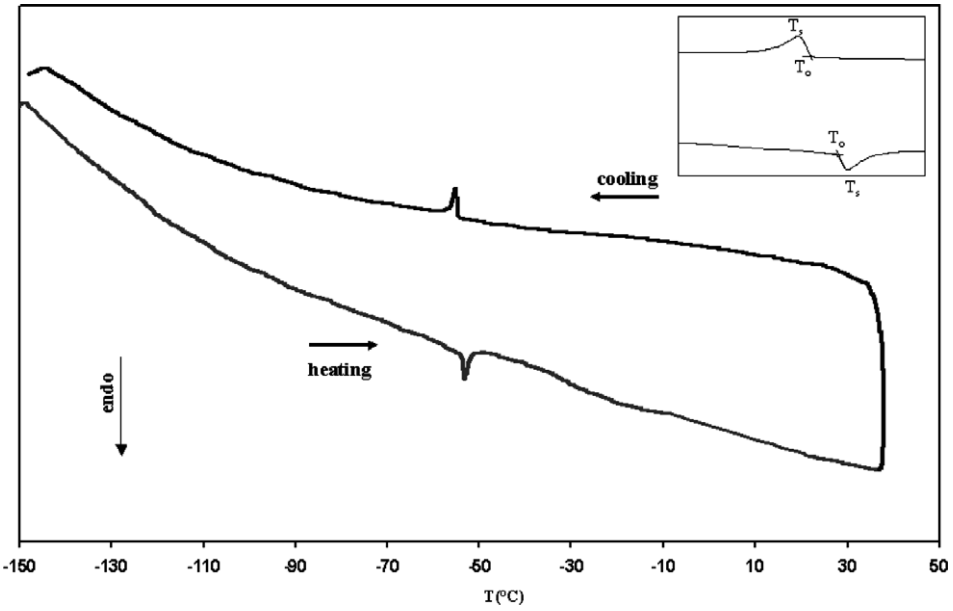

Fig. 1. DSC curves obtained upon heating and cooling for $(C_6H_{14}N_2)[Ni(H_2O)_6](SO_4)_2$ (5 °C min^{-1}).

the faces defined in the (*ac*) plane. Then, they run along the *a* and *c* axes to form organic cationic stacks along [1 0 0] and [0 0 1]. The disordered cations are isolated from one another and they alternate with the $[Ni(H_2O)_6]^{2+}$ octahedra along [1 0 1] and [0 1 0] to form mixed cationic stacks. The combination of the organic and inorganic cationic stacks leads to cationic layers parallel to the (*ac*) plane.

There is only one crystallography independent S atom with tetrahedral coordination geometry located in general position. The sulphate groups are slightly distorted with mean tetrahedral angles of 109.475° and mean S–O distance of 1.471 Å (Table 3). The oxygen atoms of each sulphate anion participate as acceptors in hydrogen bonds, for H-atoms from dabcodiium groups and water molecules.

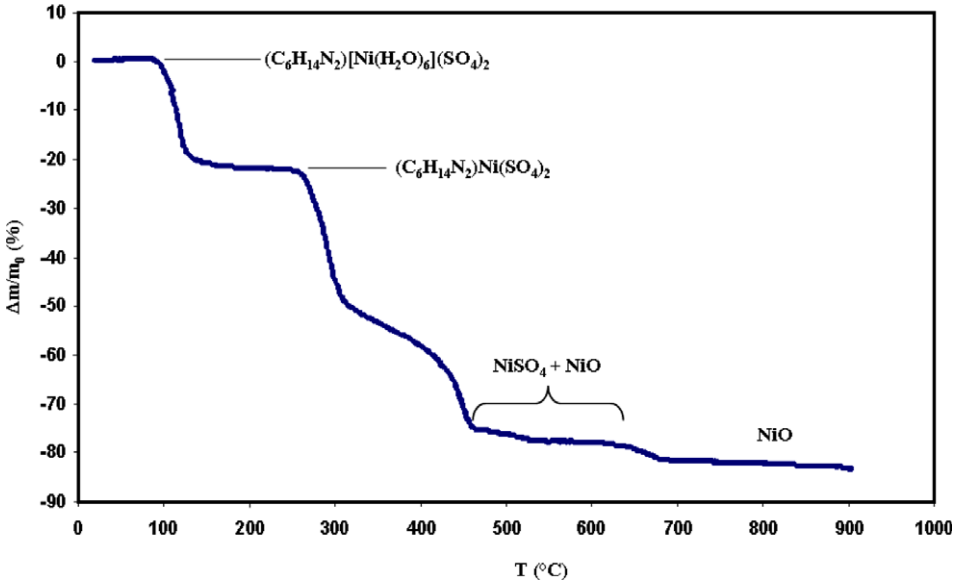

Fig. 2. TG curve for the decomposition of $(C_6H_{14}N_2)[Ni(H_2O)_6](SO_4)_2$ in air (15 °C h^{-1}).

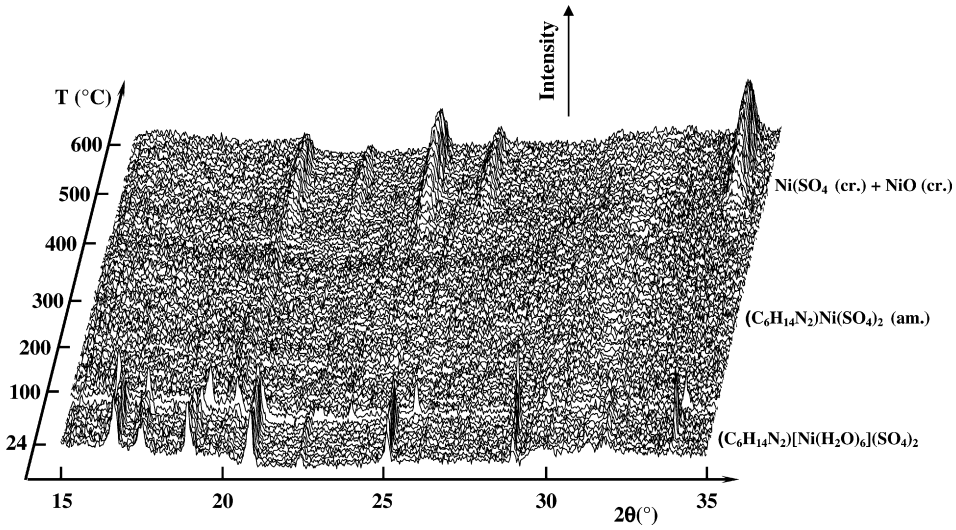

Fig. 3. TDXD plot for the decomposition of $(C_6H_{14}N_2)[Ni(H_2O)_6](SO_4)_2$ in air (7 °C h^{-1} from 18 to 610 °C; counting time of 3600 s per pattern).

The O2, O3 and O4 oxygen atoms are involved in two hydrogen bonds, each of them accepting two water hydrogen atoms, while the O1 accepts only one hydrogen bond from the organic moiety. As it can be seen in Fig. 5a, the sulphate anions play an important role in the structure connectivity. Indeed, the organic and inorganic cations are connected via hydrogen bonds, N–H···O and OW–H···O, through sulphate groups. The H···O bond length involved in the N–H···O bond has as a value 1.72(3) Å, while they fall into the range 1.81(2)–2.13(2) Å for the OW–H···O bonds, thus leading to a mean H···O value of 1.911 Å. The N···O distance is equal to 2.653(2) Å while OW···O distances vary from 2.692(2) to 2.979(2) Å (mean D···O value of 2.778 Å). Consequently, the hydrogen bonds established between the dabcodiium and the sulphate groups are stronger than those observed between water molecules and anions. The D–H···O angles range from 162(2)° to 179(2)° (mean value of 172°) (Table 4).

3.2.2. Structure of the LT-phase (determined at −173 °C)

At −173 °C, the title compound crystallises in monoclinic symmetry (space group $P2_1/a$) and exhibits a fully ordered crystal structure consisting of isolated $[Ni(H_2O)_6]^{2+}$ octahedra, SO_4^{2-} tetrahedra and dabcodiium ions linked together by a hydrogen-bonding network (Fig. 4b).

In this structure, the nickel atom occupies a general position. Its coordination polyhedron, formed by six water molecules in the form of an octahedron, is slightly irregular as seen in other templated metal sulphate [6,9,29]. Indeed, the Ni–OW distances range from 2.0310(6) to 2.1208(6) Å with a mean distance 2.066 Å (Table 3). The $Ni(OW)_6$ octahedra are isolated from each other with a shortest distance

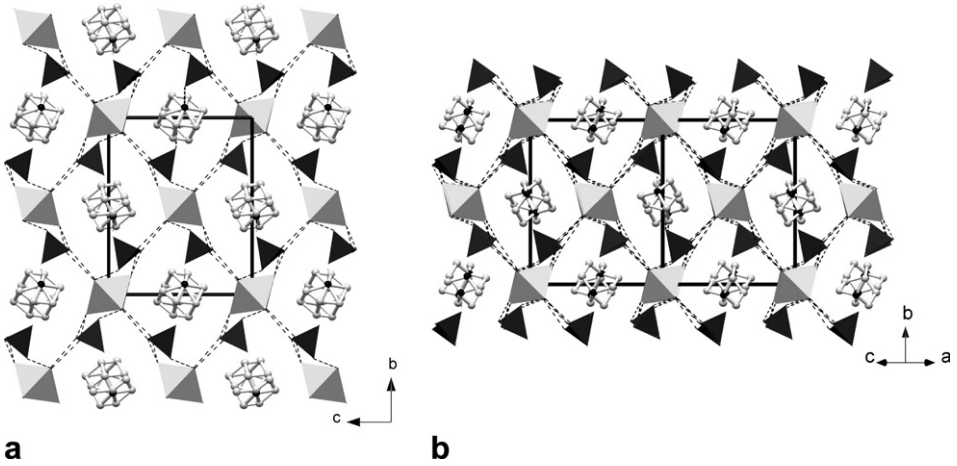

Fig. 4. Projection of the three-dimensional networks of (a) the HT-phase along the *a* axis, (b) the LT-phase along [1 0 1]. H bonds are shown as dashed lines (as in the following figures). Light grey octahedra: $[Ni(H_2O)_6]^{2+}$, dark grey tetrahedra: SO_4^{2-}, grey spheres: C, black spheres: N. H atoms are omitted for clarity.

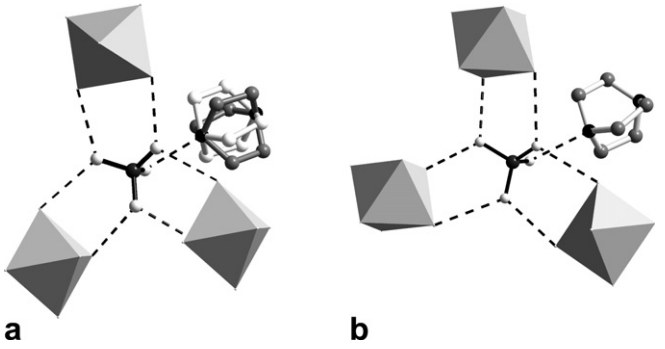

Fig. 5. Sulphate environment for (a) the HT-phase, showing the dabcodiium disorder (the two possible orientations are represented by either white C or grey C atoms), (b) the LT-phase. Note that the octahedra are not oriented in the same manner in the two phases.

Ni–Ni equal to 6.807(5) Å, which is shorter than that found in the room temperature phase (Ni–Ni = 7.0000(1) Å). The dabcodiium ordering leads to the decrease of the mean volume of the amino group. Since a dabcodiium group is located between two Ni octahedra, it is the reason of the Ni–Ni shortening. As it is observed for the HT-phase, each octahedron is H-bonded to six sulphate anions in a bidentate fashion.

Contrary to that observed for the HT-phase, the C–C and N–C distances and the C–N–C angles within the diprotonated amine (Table 3) are in agreement with these reported for $[HN(CH_2)_6NH]SO_4 \cdot 0.5H_2O$ [28], for example. The $[HN(CH_2)_6NH]^{2+}$ are stacked along the [1 0 1] direction and they are separated from one another by only one $Ni(H_2O)_6$ octahedron along *a*, *b* and *c* axes giving rise to mixed cationic layers parallel to the (*ac*) plane.

There are two crystallography distinct S atoms lying in general positions. Similarly to the $Ni(H_2O)_6$ groups, the SO_4 tetrahedra are slightly distorted, with mean tetrahedral angles of 109.47° and mean S-O bond lengths of 1.481 and 1.482 Å for $S1O_4$ and $S2O_4$, respectively (Table 3). These anions are isolated and are connected to the cations via N–H···O and OW–H···O hydrogen bonds into an extensive three-dimensional infinite framework. Within this structure, the H···O distances range from 1.75(1) to 2.10(1) Å with a mean value of 1.925 Å. The D–H···O angles are comprised in the 167(1)–179(2)° range with a mean value of 174.28° (Table 4). All O atoms belonging to the SO_4 tetrahedra are involved in two hydrogen bonds (accepting two water hydrogen atoms) with an exception for O1 and O5 which accept from only one dabcodiium H atom (Fig. 5b). As a consequence, these two S–O bonds are shorter than the others, i.e., 1.4765(6) for S1–O1 and 1.4755(6) Å for S2–O5 (Table 3).

4. Discussion

The LT- and HT-phases exhibit similar crystal structures consisting of Ni^{2+} cations octahedrally coordinated to six water molecules, sulphate tetrahedra and dabcodiium cations linked by hydrogen bonds only. However, the hydrogen bonds are stronger at −173 °C than those observed for the HT phase (Table 4), in agreement with the dabcodiium ordering and the structure freezing. The DSC shows that the title compound exhibits a reversible phase transition of the second order. The X-ray diffraction and the DSC experiments do not allow to determine the nature of the phase transition which might probably be ferroelastic-prototype as found in $(C_5H_{10}NH_2)SbCl_6 \cdot (C_5H_{10}NH_2)Cl$ crystals [30].

$[Ni(H_2O)_6]^{2+}$ and $(C_6H_{14}N_2)^{2+}$ strictly alternate in stacking directions, which differ from the LT- and HT-phases. For the HT phase (space group $P2_1/n$), the cations alternate along two directions, i.e., the *b* axis and [1 0 1]. Within similar compounds which also crystallise in space group $P2_1/n$, the stacking directions are [1 0 1/2] for the piperazine-related compound [7] and [0 0 1] for the ethylenediamine-related compound [31]. For the LT-phase (space group $P2_1/a$), the stacking directions correspond to the three cell axes *a*,

b and *c*. Within similar phases which crystallise in space group $P2_1/a$, the stacking directions correspond to the *a* and *b* axes in the guanidinium-related compound [10], and [1 0 1/0 1 1] for the ammonium Tutton's salts [32]. Although all the cited structures are similar in connectivity, it is noticeable that the alternation of the cations strongly differ from one to each other. It is likely to be the nature of the amine group that affects the positions and the orientations of the entities within the unit cell.

Such results are promising for further investigations on both the phase transition behaviour and the crystal chemistry of transition metal sulphates templated by amines.

Acknowledgements

Grateful thanks are expressed to Dr. T. Roisnel (Centre de Diffractométrie X, Université de Rennes I) and G. Marsolier for their respective assistance in single-crystal and powder X-ray diffraction data collection.

References

[1] L.F. Kirpichnikova, E.F. Andreev, N.R. Ivanov, L.A. Shuvalov, V.M. Varikash, Kristallografiya 33 (1988) 1437.
[2] A.N. Holden, B.T. Matthias, W.J. Merz, J.P. Remeika, Phys. Rev. 98 (1955) 546.
[3] N. Galesic, V.B. Jordanovska, Acta Crystallogr., Sect. C 48 (1992) 256.
[4] L.F. Kirpichnikova, L.A. Shuvalov, N.R. Ivanov, B.N. Prasolov, E.F. Andreyev, Ferroelectrics 96 (1989) 313.
[5] A. Pietraszko, K. Lukaszewicz, L.F. Kirpichnikova, Polish J. Chem. (1993) 1877.
[6] W. Rekik, H. Naïli, T. Mhiri, T. Bataille, Acta Crystallogr., Sect. E 61 (2005) m629.
[7] W. Rekik, H. Naïli, T. Bataille, T. Roisnel, T. Mhiri, Inorg. Chim. Acta 359 (2006) 3954.
[8] H. Naïli, W. Rekik, T. Bataille, T. Mhiri, Polyhedron (in press).
[9] J.-X. Pan, G.-Y. Yang, Y.-Q. Sun, Acta Crystallogr., Sect. E 59 (2003) m286.
[10] M. Fleck, L. Bohaty, E. Tillmanns, Solid State Sci. 6 (2004) 469.
[11] M.H. Ben Ghozlen, A. Daoud, Z. Kristallogr. 209 (1994) 383.
[12] A. Rujiwatra, J. Limtrakul, Acta Crystallogr., Sect. E 61 (2005) m1403.
[13] S. Chaabouni, S. Kamoun, A. Daoud, T. Mhiri, Acta Crystallogr., Sect. C 52 (1996) 505.
[14] P.C. Healy, J.M. Patrick, A.H. White, Aust. J. Chem. 37 (1984) 1105.
[15] C.N. Morimoto, E.C. Lingafelter, Acta Crystallogr., Sect. B 26 (1970) 335.
[16] V. Jordanovska, S. Aleksovska, J. Siftar, J. Thermal Anal. 38 (1992) 1563.
[17] Y.-J. Zhao, X.-H. Li, S. Wang, Acta Crystallogr., Sect. E 61 (2005) m671.
[18] I. Turel, I. Leban, M. Zupancic, P. Bukovec, K. Gruber, Acta Crystallogr., Sect. C 52 (1996) 2443.
[19] M. Rademeyer, Acta Crystallogr., Sect. E 60 (2004) m993.
[20] X.-H. Li, Q. Miao, H.-P. Xiao, M.-L. Hu, Acta Crystallogr., Sect. E 60 (2004) m1784.
[21] Y.-L. Fu, Z.-W. Xu, J.-L. Ren, S.W. Ng, Acta Crystallogr., Sect. E 61 (2005) m1639.
[22] Nonius, KappaCCD Program Software, Nonius BV, Delft, The Netherlands, 1998.
[23] Z. Otwinowski, W. Minor, C.W. Carter, R.M. Sweet (Eds.), Methods in Enzymology, vol. 276, Academic Press, New York, 1997, p. 307.
[24] J. de Meulenaer, H. Tompa, Acta Crystallogr. 19 (1965) 1014.
[25] G.M. Sheldrick, Acta Crystallogr., Sect. A 46 (1990) 467.
[26] G.M. Sheldrick, SHELXL-97: Program for Crystal Structure Refinement, University of Göttingen, Germany, 1997.
[27] J. Plévert, J.P. Auffrédic, M. Louër, D. Louër, J. Mater. Sci. 24 (1989) 1913.
[28] K. Jayaraman, A. Choudhury, C.N.R. Rao, Solid State Sci. 4 (2002) 413.
[29] G. Paul, A. Choudhury, C.N.R. Rao, Chem. Mater. 15 (2003) 1174.
[30] B. Bednarska-Bolek, A. Pietraszko, R. Jakubas, G. Bator, B. Kosturek, J. Phys.: Condens. Matter 12 (2000) 1143.
[31] P.C. Healy, J.M. Patrick, A.H. White, Austr. J. Chem. 37 (1984) 1105.
[32] E.N. Maslen, S.C. Ridout, K.J. Watson, F.H. Moore, Acta Crystallogr., Sect. C 44 (1988) 412.